Proceedings, Bicycle and Motorcycle Dynamics 2016
Symposium on the Dynamics and Control of Single Track Vehicles,
21–23 September 2016, Milwaukee, Wisconsin, USA

Buckling and dynamic collapse of the bicycle wheel

Matthew Ford*, Jim M. Papadopoulos#, Oluwaseyi Balogun†

* Department of Mechanical Engineering
Northwestern University
2145 Sheridan Road, Evanston, IL 60208, USA
e-mail: mford@u.northwestern.edu

Department of Mechanical and Industrial Engineering
Northeastern University
360 Huntington Ave., Boston, MA 02115, USA
e-mail: j.papadopoulos@neu.edu

† Department of Civil Engineering
Northwestern University
2145 Sheridan Road, Evanston, IL 60208, USA
e-mail: o-balogun@northwestern.edu

ABSTRACT

A bicycle wheel's spokes must be kept under tension to prevent them from buckling under load. However, above a certain critical tension, the rim will bend and twist out of its plane.

Keywords: bicycle wheel, buckling, bifurcation, rider safety.

1 INTRODUCTION

The bicycle wheel is a prestressed structure and is susceptible to buckling under internal forces. As the spokes are tightened uniformly, the rim deforms radially to accommodate the spoke strain. At a critical tension, the system reaches a bifurcation point and the rim buckles out of its initial plane. The post-buckling configuration is generally stable and the original shape of the wheel can be recovered by reducing the tension. Buckling can also be triggered by external forces in an otherwise stable wheel leading to a release of strain energy. This is an unstable process which generally leads to a permanently "taco-ed" wheel.

Despite its implications for wheel strength, the buckling problem has never received a rigorous treatment to our knowledge. Jobst Brandt alludes to buckling in his practical manual for wheel-builders [1]:

> "If the wheel becomes untrue in two large waves during stress relieving, the maximum, safe tension has been exceeded. Approach this tension carefully to avoid major rim distortions. When the wheel loses alignment from stress relieving, loosen all spokes a half turn before retruing the wheel."

He did not discuss the problem further, but suggested that wheel failure commonly occurs due to a loss of lateral stability caused by spoke buckling. Pippard and Francis [2] derived a model for lateral stiffness based on the elastic foundation model, but did not discuss stability and neglected any effects of spoke tension.

The bicycle wheel can be modeled as an elastically supported arch in which the included angle is allowed to go to 2π. Timoshenko and Gere [3] gave a formula for the critical load for a ring with doubly-symmetric cross-section subjected to radial loads. The theory of flexural-torsional buckling of monosymmetric arches (bicycle rims have only one plane of symmetry) was broadly formalized by Trahair and Papangelis [4] using the virtual work approach to derive the equilibrium and stability equations. Their theory has been extended to treat arches restrained by continuous [5] or discrete [6] elastic supports and elastic end restraints [7].

The problem of the prestressed bicycle wheel is unique for a number of reasons. First, the buckling load is internal to the structure. Second, the spokes act both as elastic restraints resisting buckling and as prestressing elements causing buckling. Third, the lateral, radial, and torsional restraining actions of the spokes are coupled—i.e. lateral deflection at a spoke may produce lateral, radial, and torsional reactions. These considerations extend to other structural systems. Large observation wheels such as the London Eye [8] and the Singapore Flyer [9] resemble large bicycle wheels and achieve lateral stability due to the bracing angle of prestressed cables, and must be designed against flexural-torsional buckling.

Here we derive a simple solution for buckling of a spoked bicycle wheel under self-tension and investigate several special cases.

2 DEFORMATION OF THE WHEEL

A typical bicycle wheel (Fig. 1 consists of a slender rim connected to a hub by means of a system of very slender metal spokes. The spokes are usually threaded at the rim side into spoke nipples which are inserted through the rim from the outside. The spokes are kept under tension by the rim. Without pretension, the spokes would immediately buckle under a very small load due to their high aspect ratio.

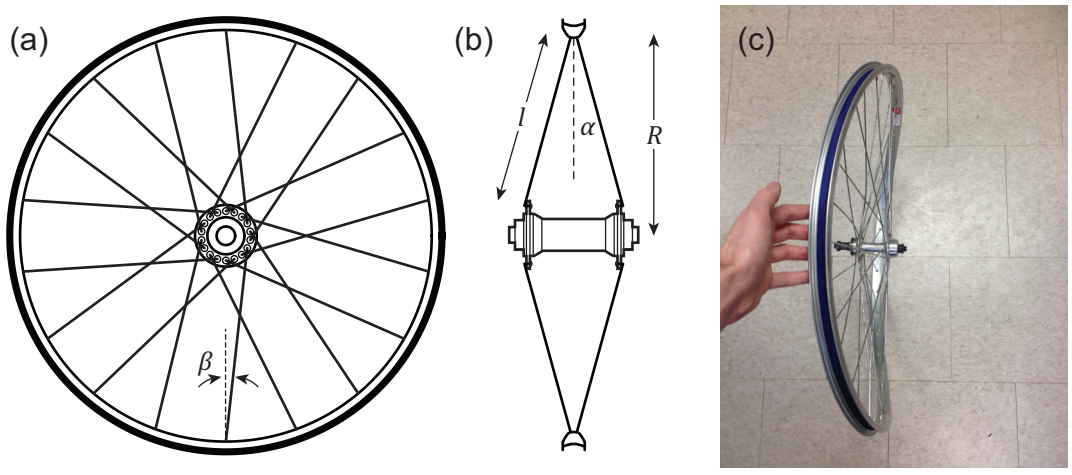

Figure 1. **(a)**-**(b)** Schematic of a model bicycle wheel. In general, the spokes lie on a hyperboloid which forms an angle of α with the wheel plane. If the in-plane angle β is zero, the spoke surface is precisely a cone. **(c)** A wheel buckled into a saddle shape.

To hold the spokes under tension, the rim must be under compression. An accurate approximation[1]

[1] 95% accurate for 6 spokes, $\alpha = 10°$, $\beta = 10°$. Increasing the number of spokes only improves the estimate.

was given by Sharp [10] by considering a force balance on the top (or bottom) half of the rim.

$$N_r = \frac{n_s T}{2\pi} \tag{1}$$

The spokes act like guy-wires, both supporting the rim radially and stabilizing the rim laterally. However, if the spoke tension exceeds a critical value T_c, the compression in the rim causes the wheel to buckle laterally, bending and twisting out of its initial plane, as shown in Fig. 1 (c).

2.1 Rim equations

The rim is modeled as an initially circular beam with a constant cross-section. For simplicity we will assume that the shear center and centroid of the cross-section coincide. Except for warping deformation, plane cross-sections remain planar and shear flexibility of the cross-section is neglected. Furthermore, we assume that the rim radius is much larger than the height of the rim profile.

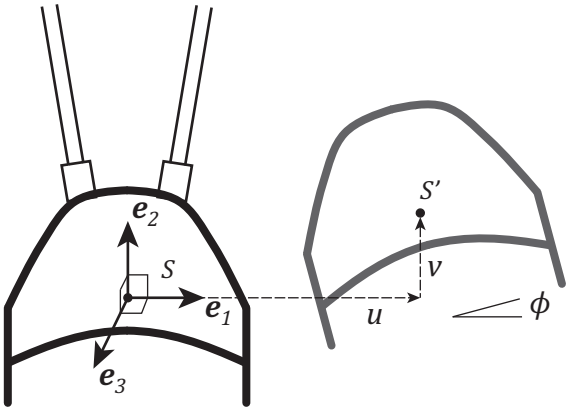

Figure 2. Deformation of a rim cross-section. The shear center $S \rightarrow S'$ translates by the vector $\boldsymbol{u} = u\hat{\boldsymbol{e}}_1 + v\hat{\boldsymbol{e}}_2 + w\hat{\boldsymbol{e}}_3$ and rotates through an angle ϕ.

The in-plane curvature κ_1 is assumed to remain constant during flexural-torsional buckling. The in-plane curvature, out-of-plane curvature and twist rate are

$$\kappa_1 = 1/R \tag{2}$$

$$\kappa_2 = u'' - \frac{\phi}{R} \tag{3}$$

$$\kappa_3 = \phi' + \frac{1}{R}u' \tag{4}$$

The symbol $()'$ indicates a derivative with respect to s. It can easily be verified that Equations 3 and 4 simplify to the standard equations for straight beams in the limit $R \rightarrow \infty$. The curvature and twist rate produce a bending moment and twisting moment equal to

$$M_2 = EI_{11}\kappa_2 \tag{5}$$

$$M_3 = GJ\kappa_3 + EI_w\kappa_3'' \tag{6}$$

The total strain energy is decomposed into lateral bending, uniform torsion, and warping terms which are related to the curvatures.

$$U_{rim} = \int_0^{2\pi} \left(\frac{1}{2} EI_{22} \kappa_2^2 + \frac{1}{2} GJ \kappa_3^2 + \frac{1}{2} EI_w (\kappa_3')^2 \right) ds \tag{7}$$

After buckling, a differential line segment ds deforms to dS. The apparent shortening of the line segment along the s direction is then

$$ds - dS = ds - \sqrt{ds^2 - \left(\frac{du}{ds} ds \right)^2} \approx \frac{1}{2} (u')^2 \, ds \tag{8}$$

The axial compressive force in the rim moves through this differential displacement, performing virtual work equal to

$$V_{rim} = \frac{1}{2} \int_0^{2\pi} N_r (u')^2 \, ds \tag{9}$$

2.2 Spoke equations

In this paper we consider bicycle wheels with slender prestressed spokes. We model a single spoke as an elastic bar pinned at each end. This ensures that the spoke force is always collinear with the spoke axis. We fix our global coordinate system to the hub, which is assumed to be rigid. Therefore, the displacement of the hub node of a spoke is zero. The linearized elongation of a spoke is given by

$$\Delta l = \boldsymbol{u}_n \cdot \hat{\boldsymbol{n}}_1 \tag{10}$$

where $\boldsymbol{u}_n$ is the displacement vector of the spoke nipple and $\hat{\boldsymbol{n}}_1$ is a unit vector pointing from the spoke nipple to the hub eyelet. The linearized rotation of the spoke is given by

$$\Omega_1 = \frac{1}{l} \boldsymbol{u}_n \cdot \hat{\boldsymbol{n}}_2 \tag{11}$$

$$\Omega_2 = \frac{1}{l} \boldsymbol{u}_n \cdot \hat{\boldsymbol{n}}_3 \tag{12}$$

where $\hat{\boldsymbol{n}}_2$ and $\hat{\boldsymbol{n}}_3$ are two orthogonal unit vectors orthogonal to $\hat{\boldsymbol{n}}_1$, and l is the spoke length.

The elongation produces a net force on the rim parallel to the original spoke axis equal to

$$f_1 = E_s A_s \left(\frac{\Delta l}{l} \right) \hat{\boldsymbol{n}}_1 = \frac{E_s A_s}{l} \hat{\boldsymbol{n}}_1 \cdot \boldsymbol{u}_n \tag{13}$$

The rotation of the spoke produces net forces on the rim perpendicular to the original spoke axis due to the rotation of the initial tension vector.

$$f_2 = T \sin \Omega_1 \approx \frac{T}{l} \hat{\boldsymbol{n}}_2 \cdot \boldsymbol{u}_n \tag{14}$$

$$f_3 = T \sin \Omega_2 \approx \frac{T}{l} \hat{\boldsymbol{n}}_2 \cdot \boldsymbol{u}_n \tag{15}$$

since $\hat{\boldsymbol{n}}_1$, $\hat{\boldsymbol{n}}_2$, $\hat{\boldsymbol{n}}_3$ are mutually orthogonal, the total force on the rim is given by $\boldsymbol{f} = \boldsymbol{k}_f \cdot \boldsymbol{u}_n$, where the spoke stiffness matrix is given by

$$\boldsymbol{k}_f = \frac{E_s A_s}{l} \hat{\boldsymbol{n}}_1 \hat{\boldsymbol{n}}_1 + \frac{T}{l} (\hat{\boldsymbol{n}}_2 \hat{\boldsymbol{n}}_2 + \hat{\boldsymbol{n}}_3 \hat{\boldsymbol{n}}_3) \tag{16}$$

The first term in Eqn. 16 is the **elastic stiffness** and the second term is the **tension stiffness**. The tension stiffness is the component responsible for the transverse vibrations of a guitar string, e.g.

Following the approach of Smith [11] and Pippard [2], we will approximate the spoke system as a continuum which exerts a distributed load on the rim. The stiffness per unit length is defined by the sum of the spoke stiffnesses in one periodic grouping of n_p spokes, divided by the arc length of the grouping.

$$\bar{\boldsymbol{k}} = \frac{1}{2\pi R}\left(\frac{n_s}{n_p}\right)\sum_{i}^{n_p}\boldsymbol{k}_{f,i} \tag{17}$$

The distributed load $\bar{\boldsymbol{f}}$ does an amount of work per unit length equal to

$$\bar{w} = \int_0^{u_n} \bar{\boldsymbol{f}} \cdot d\boldsymbol{u}_n = \frac{1}{2}\boldsymbol{u}_n \cdot \bar{\boldsymbol{k}} \cdot \boldsymbol{u}_n \tag{18}$$

The line of action is assumed to pass sufficiently close to the rim shear center that any difference between the displacement of the spoke nipple and the displacement of the shear center can be ignored. Therefore $\boldsymbol{u}_n = \boldsymbol{u}$. Substituting a lateral buckling displacement $\boldsymbol{u} = u\hat{\boldsymbol{e}}_1$ into Eqn. 18 and integrating over the length of the rim gives the strain energy stored in the spoke system.

$$U_{spokes} = \int_0^{2\pi} \bar{w}\, ds = \frac{1}{2}\bar{k}_{uu}u^2 \tag{19}$$

The continuum spoke stiffness can be written $\bar{\boldsymbol{k}} = \bar{\boldsymbol{k}}^{el} + T\bar{\boldsymbol{k}}^{tens}$, where the dependence on T is shown explicitly. A very close approximation for the $\bar{k}_{uu}$ component for a symmetrically dished wheel is given by

$$\bar{k}_{uu} = \frac{n_s E_s A_s}{2\pi R l}\sin^2\alpha + \frac{n_s T}{2\pi R l} \tag{20}$$

2.3 Total potential energy and buckling criterion

The buckled shape of the wheel must be periodic, so we assume a buckled shape of the form

$$\begin{aligned} u &= \delta u_n \cos\frac{ns}{R} \\ \phi &= \delta\phi_n \cos\frac{ns}{R} \end{aligned} \tag{21}$$

The wheel becomes unstable when the increase in strain energy is exactly balanced by the virtual work for a perturbing displacement $\delta u_n, \delta\phi_n$, i.e. when the total potential energy is zero.

$$\Pi = U_{rim} + U_{spokes} - V_{rim} = 0 \tag{22}$$

Substituting the buckling mode shape Eqn. 21 into Eqns. 7, 9, and 19 and substituting into Eqn. 22 yields a buckling criterion for the nth mode.

$$\frac{\pi E I_{11}}{R^3}(n^2u_n - R\phi_n)^2 + \frac{\pi n^2}{R^2}\left(GJ + \frac{EI_w}{R^2}n^2\right)(u_n - R\phi_n)^2 + \pi R(\bar{k}^{el}_{uu} + T\bar{k}^{el}_{uu})u_n^2 - N_r\frac{\pi n^2}{R}u_n^2 = 0 \tag{23}$$

The torsional rigidity and warping rigidity can be combined into an effective torsional stiffness $\widetilde{GJ} = GJ + n^2EI_w/R^2$. Equation 23 has a quadratic form and can be written using matrix notation:

$$\begin{bmatrix} u_n \\ \phi_n \end{bmatrix} \cdot \begin{bmatrix} \frac{\partial^2\Pi}{\partial u_n^2} & \frac{\partial^2\Pi}{\partial u_n \partial\phi_n} \\ \frac{\partial^2\Pi}{\partial u_n\partial\phi_n} & \frac{\partial^2\Pi}{\partial\phi_n^2} \end{bmatrix} \cdot \begin{bmatrix} u_n \\ \phi_n \end{bmatrix} = 0 \tag{24}$$

Non-trivial solutions of Eqn. 24 exist when the determinant of the matrix vanishes. Expanding the determinant in Eqn. 24 and substituting Eqn. 1 yields a linear equation for the critical buckling tension of the nth mode.

$$\left(\frac{2\pi EI_{22}}{R}+\frac{2\pi\widetilde{GJ}n^2}{R}\right)\left(\frac{2\pi\widetilde{GJ}n^2}{R^3}+\frac{2\pi EI_{22}n^4}{R^3}+2\pi R\bar{k}_{uu}^{el}+\frac{n_sT_{cn}}{l}-\frac{n_sn^2T_{cn}}{R}\right)$$
$$-\left(\frac{2\pi EI_{22}n^2}{R^2}+\frac{2\pi\widetilde{GJ}n^2}{R^2}\right)^2=0 \quad (25)$$

Solving Eqn. 25 for T_{cn} yields the tension at which the nth mode becomes unstable. The critical buckling tension T_c is the minimum T_{cn} with respect to the mode number $n \geq 2$.

3 BUCKLING DUE TO SPOKE TENSION

The solution to Eqn. 25 can be written in non-dimensional form as

$$\frac{T_{cn}}{T_e}=\left(\frac{\tilde{u}n^2(n^2-1)^2}{1+\tilde{\mu}n^2}+\lambda\right)\left(\frac{1}{n^2-1}\right) \quad (26)$$

where the "Euler tension" $T_e = 2\pi EI_{22}/n_sR^2$ is the tension that would produce a compressive force in the rim equal to the classical buckling load for a straight beam-column of length $2\pi R$. The parameter $\tilde{\mu} = \widetilde{GJ}/EI_{22}$ is the ratio of the effective torsional stiffness to the lateral bending stiffness. The parameter $\lambda = \bar{k}_{uu}^{el}R^4/EI_{22}$ is the ratio of the spoke system stiffness $\bar{k}_{uu}^{el}R$ to the rim bending stiffness EI_{22}/R^3.

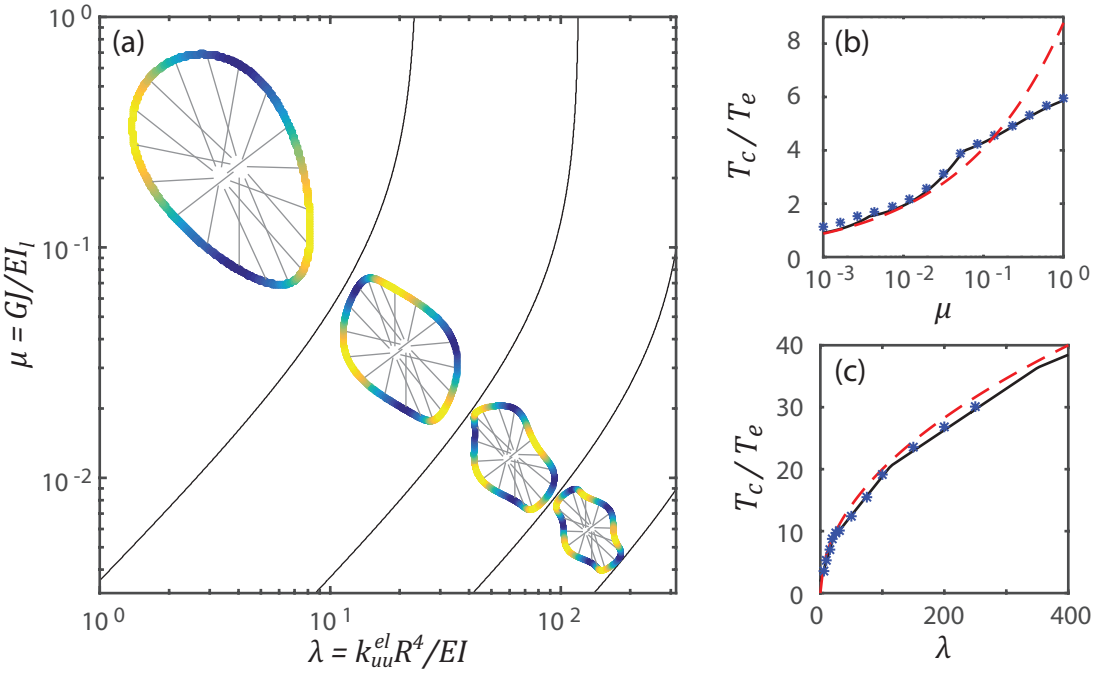

Figure 3. **(a)** Buckling mode parameter map. Only the first 4 modes are shown. **(b)–(c)** Normalized buckling tension vs. $\tilde{\mu}$ and λ. Solid black line = Eqn. 26, dashed red line = power law, blue stars = finite-element simulations. In (a) $\lambda = 10$ while in (b) $\tilde{\mu} = 0.38$.

Since n is a discrete variable, there is no closed-form for the minimum T_{cn} for a given $(\tilde{\mu}, \lambda)$. However, two important *approximate* solutions can be derived by replacing the discrete n with a continuous variable $\bar{n}$ and minimizing Eqn. 26 analytically, resulting in two simple power laws for T_c.

3.1 Rims with low torsional stiffness

Many bicycle rims are built from thin-walled open channels which have very low torsional stiffness compared with their bending stiffness. Replacing the discrete mode number n with a continuous variable $\bar{n}$, we adopt the following ansatz: (a) $\bar{n}^2 \gg 1$ and (b) $\tilde{\mu}\bar{n}^2 \ll 1$. Under these conditions, Eqn. 26 becomes

$$T_{cn} = \frac{2\pi E I_{11}}{n_s R^2}\left(\tilde{\mu}\bar{n}^4 + \frac{\lambda}{\bar{n}^2}\right) \tag{27}$$

Minimizing Eqn. 27 with respect to $\bar{n}$ by setting the derivative $dT_{cn}/d\bar{n} = 0$, we obtain the scaling law

$$\bar{n} = \left(\frac{\lambda}{2\tilde{\mu}}\right) \tag{28}$$

Substituting Eqn. 28 into Eqn. 29 yields, after simplification, a simple power law relationship.

$$T_c \approx \frac{11.875}{n_s R^2}\left(\bar{k}_{uu}^{el} R^4\right)^{2/3} (\widetilde{GJ})^{1/3} \tag{29}$$

Equation 29 suggests that when the torsional stiffness is smaller than the bending stiffness, the buckling behavior is dominated by torsion and does not depend explicitly on the bending stiffness at all. Equation 29 is shown in Fig. 3 next to Equation 26 and finite-element calculations. The power law is strictly less than Equation 26 which conveniently gives a conservative design criterion.

3.2 Spokes much stiffer than the rim

A second power law regime appears when $\lambda \gg 1$ and $\tilde{\mu} \sim 1$. Under these conditions, Eqn. 26 becomes

$$T_{cn} = \frac{2\pi E I_{11}}{n_s R^2}\left(\bar{n}^2 + \frac{\lambda}{\bar{n}^2}\right) \tag{30}$$

Following the same procedure in section 3.1 gives a separate power law, after simplification.

$$T_c \approx \frac{4\pi}{n_s}\left(\bar{k}_{uu}^{el} E I_{11}\right)^{1/2} \tag{31}$$

Substituting Eqn. 1 for T_c gives $N_{rc} = 2\sqrt{\bar{k}_{uu}^{el} E I_{11}}$, which is precisely the buckling load for an infinite, straight beam on an elastic foundation [12]. Figure 3 (c) shows a comparison of Eqn. 31 against Eqn. 26 and finite-element calculations.

4 EQUIVALENT SPRING MODEL

The lateral stiffness of the wheel can be decomposed into orthogonal modes in the form of Eqn. 21. Since the Fourier modes are orthogonal, the total strain energy is the sum of the strain energy in each mode.

$$U_{total} = U_0 + U_1 + U_2 + ... \tag{32}$$

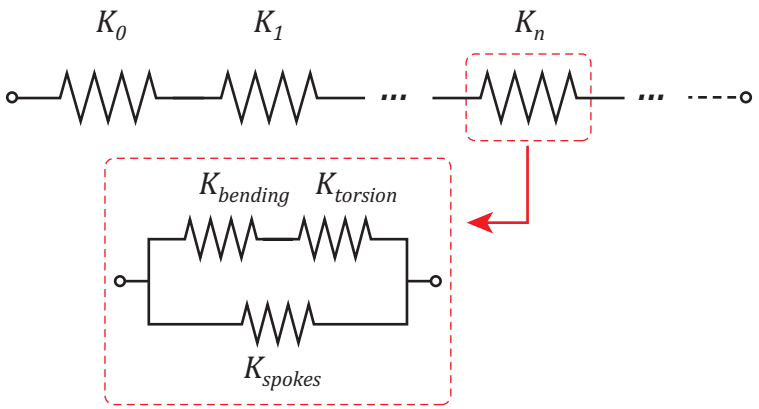

Figure 4. Equivalent spring model. Each mode stiffness consists of three equivalent springs representing the rim bending and torsion stiffness and the spoke stiffness.

The applied lateral force and torque are determined using Castigliano's first theorem. For an applied force P and no applied torque, we have

$$\begin{aligned} P &= \frac{\partial U_n}{\partial u_n} \\ 0 &= \frac{\partial U_n}{\partial \phi_n} \end{aligned} \tag{33}$$

Substituting $U_{rim} + U_{spokes}$ for U_n and inserting the mode shape Eqn. 21, Eqn. 33 becomes a linear system of equations for u_n and ϕ_n. Solving 33 for u_n yields

$$u_n = \left(\frac{PR^3}{\pi}\right) \frac{EI_{11} + \widetilde{GJ}n^2}{EI_{11}\widetilde{GJ}n^2(n^2-1)^2 + R\bar{k}_{uu}(EI_{11} + \widetilde{GJ}n^2)} \tag{34}$$

The stiffness of the nth mode is then defined as

$$K_n = P/u_n = \left(\frac{\pi}{R^3}\right) \frac{EI_{11}\widetilde{GJ}n^2(n^2-1)^2}{EI_{11} + \widetilde{GJ}n^2} + \pi R\bar{k}_{uu} \tag{35}$$

Defining an equivalent torsion stiffness, bending stiffness, and spoke stiffness, Eqn. 35 can be written succinctly as

$$K_n = \frac{K_{bending}K_{torsion}}{K_{bending} + K_{torsion}} + K_{spokes} \tag{36}$$

where

$$K_{torsion} = \widetilde{GJ}n^2\frac{\pi(n^2-1)^2}{R^3} \tag{37}$$

$$K_{torsion} = EI_{11}\frac{\pi(n^2-1)^2}{R^3} \tag{38}$$

$$K_{spokes} = \pi R\bar{k}_{uu} \tag{39}$$

The form of Equation 36 suggests an equivalent spring model (Fig. 4) for the nth mode in which the rim stiffness is represented by two springs connected which is then connected in parallel with

the spoke stiffness. If there is a large difference between the rim bending stiffness and torsion stiffness, the equivalent rim stiffness will be dominated by the smaller of the two.

With this definition, Eqn. 26 has an extremely simple form

$$T_{cn} = \frac{2R}{n_s(n^2 - R/l)} K_n \tag{40}$$

In this form, the benefit of adding spoke stiffness becomes readily apparent. Because the rim stiffness and spoke stiffness act in parallel, increasing either one directly impacts the maximum tension.

5 FINITE-ELEMENT MODEL

We validated our theoretical predictions using non-linear finite-element calculations implemented in ABAQUS® 6.14[2]. The spokes and rim were both modeled using 2-node linear beam elements including shear flexibility (element type B31 in the ABAQUS library). The rim was interpolated with sufficient elements such that any given beam segment spanned less than 6° of the circle.

A controlled eigenstrain was applied to the spokes by defining a coefficient of thermal expansion of 1.0 for the spokes (but not the rim) and ramping the temperature down to 150% of the expected critical buckling strain. Mesh imperfections of the form $\cos ns/R$ were added to perturb the initial lateral positions of the rim nodes. Modes starting with $n = 2$ up to the expected buckling mode were included. The ABAQUS Standard static solution procedure was used with non-linear geometric effects.

The average spoke tension was recorded at each time step. The buckling tension was determined from a Southwell plot [3] of u/T vs. u, where u is taken at its maximum location on the rim. The deflection of a loaded structure with an initial imperfection is (to first order)

$$u = \frac{a}{T_c/T - 1} \tag{41}$$

Therefore the slope of u/T vs. u is $1/T_c$. The buckling tension was also calculated by finding the strain at which the average tension departs from linearity by more than 3%. The two methods were found to give results in very close agreement.

6 CONCLUSIONS

...

REFERENCES

[1] Brandt, J. The Bicycle Wheel (Avocet, Palo Alto, CA, 1993), 3rd edn.

[2] Pippard, A. S. & Francis, W. The Stresses in a Wire Wheel under Side Loads on the Rim. Philos. Mag. **14**, 436–445 (1932).

[3] Timoshenko, S. P. & Gere, J. M. Theory of Elastic Stability (McGraw-Hill, New York, NY, 1961), 2nd edn.

[2] ABAQUS® is a registered trademark of Dassault Systèmes.

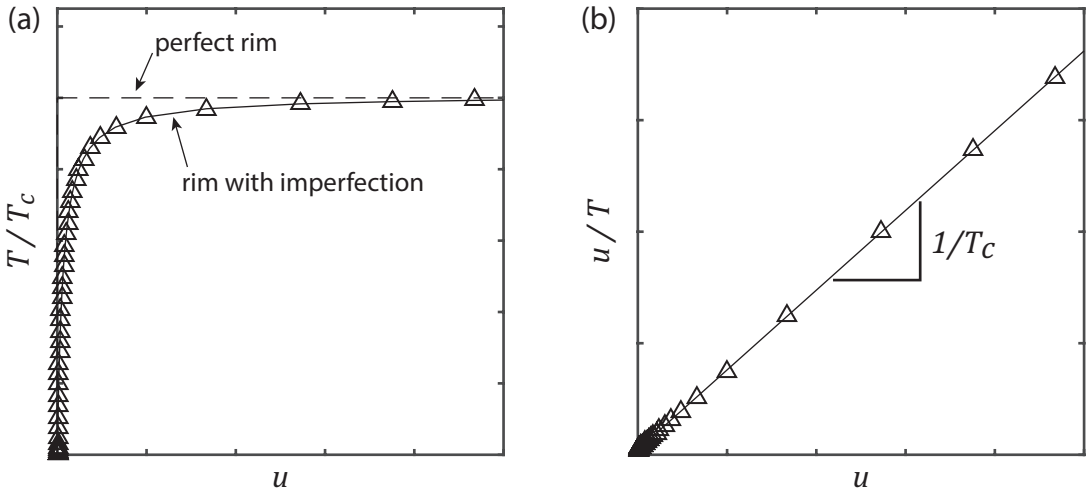

Figure 5. **(a)** Normalized spoke tension vs. lateral deflection. **(b)** Southwell plot.

[4] Trahair, N. S. & Papangelis, J. P. Flexural-torsional buckling of monosymmetric arches. J. Struct. Eng. **113**, 2271–2288 (1987).

[5] Pi, Y.-L. & Bradford, M. Elastic flexural-torsional buckling of continuously restrained arches. Int. J. Solids Struct. **39**, 2299–2322 (2002).

[6] Bradford, M. A. & Pi, Y.-L. Elastic Flexural-Torsional Buckling of Discretely Restrained Arches. J. Struct. Eng. **128**, 719–727 (2002).

[7] Guo, Y. L., Zhao, S. Y., Dou, C. & Pi, Y. L. Out-of-Plane Elastic Buckling of Circular Arches with Elastic End Restraints. J. Struct. Eng. **140**, 9 (2014).

[8] Mann, A., Thompson, N. & Smits, M. Building the British Airways London Eye. Proc. Inst. Civ. Eng. - Civ. Eng. **144**, 60–72 (2001).

[9] Allsop, A., Dallard, P. & McNiven, B. The Singapore Flyer and Design of Giant Observation Wheels, Singapore. Struct. Eng. Int. **19**, 12–16 (2009).

[10] Sharp, A. Bicycles and Tricycles (MIT Press, Cambridge, MA, 1977), 2nd edn.

[11] Smith, B. A. The Bicycle Wheel. Rep. Aust. As. **8**, 197–203 (1901).

[12] Hetenyi, M. Beams on elastic foundation (Univ. of Michigan Press, Ann Arbor, MI, 1946).

LIST OF TERMS

The following notation is used in this paper:

Term	***Definition***
n_s	Number of spokes
E_s, A_s	Spoke Young's modulus and cross-sectional area
l	Spoke length
α	Out-of-plane spoke angle–wall angle of a hypothetical "cone" of spokes
β	In-plane spoke angle–measured between the in-plane projection of the spoke and a radius of the wheel
$\hat{\boldsymbol{n}}_1$	Unit vector aligned with the spoke axis
$\hat{\boldsymbol{n}}_2, \hat{\boldsymbol{n}}_3$	Two unit vectors perpendicular to the spoke axis
$\hat{\boldsymbol{e}}_1, \hat{\boldsymbol{e}}_2, \hat{\boldsymbol{e}}_3$	Coordinate axes defined at the rim shear center
$\boldsymbol{u}$	Displacement of the rim shear center
u, v, w	Vector components of $\boldsymbol{u}$ in the $\hat{\boldsymbol{e}}_1$, $\hat{\boldsymbol{e}}_2$, $\hat{\boldsymbol{e}}_3$ directions.
ϕ	Rotation of the rim cross-section about the $\hat{\boldsymbol{e}}_3$ axis.
$\delta u, \delta\phi$	Virtual displacement and rotation
u_n, ϕ_n	Buckling mode coefficients
n	Buckling mode number
T	Tension in a spoke
T_{cn}	Critical tension for the nth mode
T_c	Critical buckling tension (minimum of T_{cn} over all modes)
T_e	"Euler" tension–tension which would produce an axial force in the rim equal to the buckling load for a straight beam-column of length $2\pi R$
$\boldsymbol{f}$	Force exerted by a spoke on the rim
f_1, f_2, f_3	Vector components of $\boldsymbol{f}$
$\boldsymbol{k}_f$	Stiffness matrix for a single spoke
$\bar{\boldsymbol{k}}$	Equivalent stiffness per-unit-length of the spoke system. $\bar{\boldsymbol{k}} = \bar{\boldsymbol{k}}^{el} + \bar{\boldsymbol{k}}^{tens}$
$\bar{\boldsymbol{k}}^{el}$	Part of $\bar{\boldsymbol{k}}$ proportional to $E_s A_s$
$\bar{\boldsymbol{k}}^{tens}$	Part of $\bar{\boldsymbol{k}}$ proportional to T
$\bar{k}_{ij}$	Tensor components of $\bar{\boldsymbol{k}}$
R	Rim radius–measured from the rim shear center
E	Rim Young's modulus
I_{11}	Second moment of area of the rim in the lateral direction
J	Rim torsion constant
I_w	Rim warping constant
$\widetilde{GJ}$	Effective torsional rigidity including both Saint-Venant torsion and warping
$\tilde{\mu}$	Ratio of effective torsional rigidity to bending rigidity: $\widetilde{GJ}/EI_{11}$
λ	Ratio of spoke system stiffness to rim bending stiffness OR ratio of rim radius to the characteristic length of a beam on an elastic foundation.